ZEPHAL

Titre:

Cooling System Design and Simulation – Part 1

Rédacteur :

Quentin Rousse

Signataire :

/

Révision :

A1 – Edition initiale

Zephal Technologies

NZ-00000003

Date :	05/01/2026
N° de projet :	2025_0004

Introduction

Purpose of the cooling system

The V1046AA develops 680 hp at 10,500 rpm, or 500 kW. The total power contained in the fuel consumed is estimated at 3x this value, or 1,500 kW. Of this 1,500 kW, the total power absorbed by the cooling systems is estimated at 420 kW. It is estimated that approximately 65% of this power will be dissipated in the cooling circuit, with the remainder being evacuated in the oil system and through radiation.

We therefore have 273 kW to dissipate. However, as this figure is an estimate, a 20% increase in the power to be dissipated is applied, bringing the dissipation requirement to 327 kW.

To have an engine that is easy to maintain and use daily, a conventional cooling additive, G13, is added to the water in equal proportions (50/50).

The characteristics of this mixture are as follows:

Property	***Value***	***Unit***
Density (ρ)	1065	Kg/m^3
Specific heat capacity (Cp)	3,45	J/(g.K)
Dynamic viscosity (μ)	1,8	mPa.s
Thermal conductivity (λ)	0,42	W/(m.K)
Ebullition point (1 bar)	108	°C
Ebullition point (2 bars)	125	°C

In the previous article, *Development of a new V10 engine – an introduction*, on page 9, we determined the flow rate required by the system to absorb the power: 267 L/min. To compensate for pressure losses in the circuit, the objective is to develop a water pump capable of generating approximately 2.5 bars of overpressure (~25 m HMT). These losses are estimated based on similar engines at this stage of development, as the true value of system pressure losses is virtually impossible to determine using numerical methods due to the number of parameters involved and the uncertainty surrounding them (tolerances, roughness, actual geometry, etc.).

In the rest of this article, we will focus on two points: First, modeling and analyzing the water distribution channel to the cylinders, verifying that the distributed pressure is uniform between the cylinders and that there are no significant pressure losses. Second, we will design the water pump, from theory to mechanical assembly, with a dimensioning sequence performed using the OpenFoam CFD library.

Note: In this document, "water" and "coolant" are used interchangeably for the sake of brevity.

Toute information contenue dans ce document est libre d'être diffusée à des tierces parties.

Conception and simulation of the Water Channel

The design choices made for the engine block led to the use of an external water channel attached to the assembly. This channel must ensure optimal water distribution to each cylinder, i.e., limit pressure losses and limit the pressure differential between each cylinder inlet.

Initial design

The space reserved for the channel on the block consists of 10 outlets (in red) and one inlet (in green). It is secured using two M6 screws on each cylinder and two M8 screws on the water inlet. Each interface is sealed using a flat gasket.

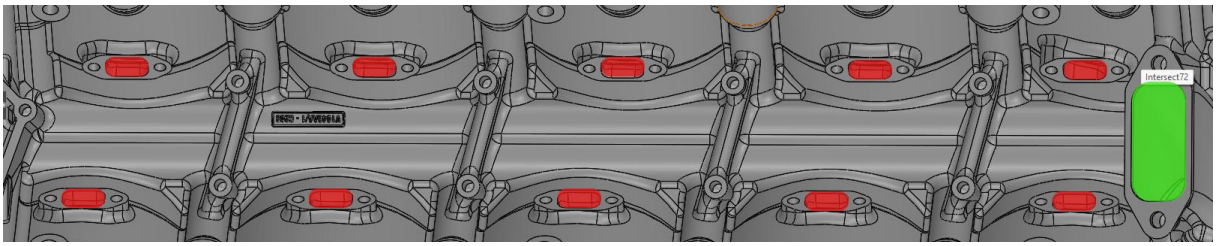


Figure 1: Fixation points for the water channel

The initial design was as follows: a channel of sufficient length to reach all cylinders with outlets connecting to each cylinder, including pockets for using M6 CHC screws. Water enters via an inlet channel that “spills” between the first four cylinders. The center of the channel is gradually hollowed out to prevent excessive fluid stagnation. Any doubts regarding potential pressure losses caused by these pockets were dispelled by CFD flow analysis.

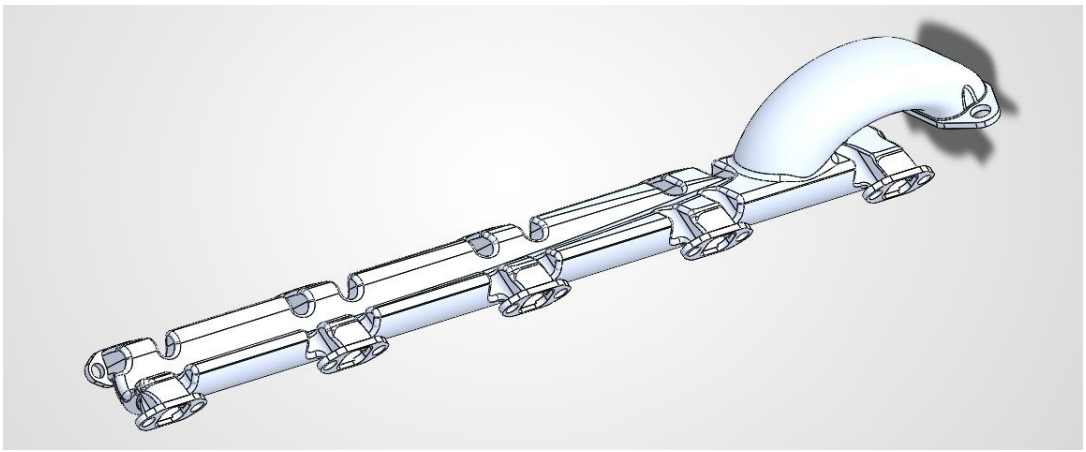


Figure 2: 3D model of the water channel

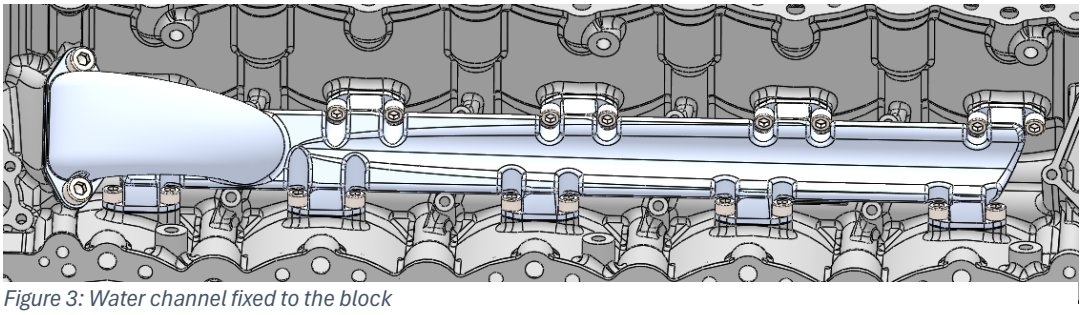


Figure 3: Water channel fixed to the block

Toute information contenue dans ce document est libre d'être diffusée à des tierces parties.

Validation in CFD

Simulation objectives

The channel has a critical function: to bring coolant to the cylinders and ensure sufficient flow to each cylinder. In other words, the pressure of the liquid in each of the 10 outlets must be the same, with a maximum deviation of 5%.

The criterion of a maximum pressure differential of 5% between cylinder inlets was chosen to ensure even distribution of the coolant flow.

In turbulent flow conditions, which is the case for the circuit studied, the flow rate is proportional to the square root of the pressure differential. Thus, a pressure difference of 5% results in a flow imbalance of around 2 to 3% between cylinders.

This implies two criteria to be validated:

- The absence of “dead zones”: recirculation, excessive pressure drops, etc.
- The pressure differential between each outlet of the channel

The simulation will use a mesh generated using SALOME software, followed by an OpenFoam simulation with the SimpleFoam solver, incorporating turbulence and a surface roughness of 63 µm, which is representative, or even overestimated, of a cast or 3D-printed metal part.

Meshing in SALOME

After creating the CFD domain in Solidworks, corresponding to the internal space of the channel, the mesh was generated according to the following parameters (sizes in mm):

Dimension	Algorithm	Max. size	Min. size
3D	NETGEN 3D	0.003	0.0005
2D	NETGEN 2D-1D	0.003	0.0005
1D	NETGEN 2D-1D	0.003	0.0005

Local refining of 0.001 on the walls was also used.

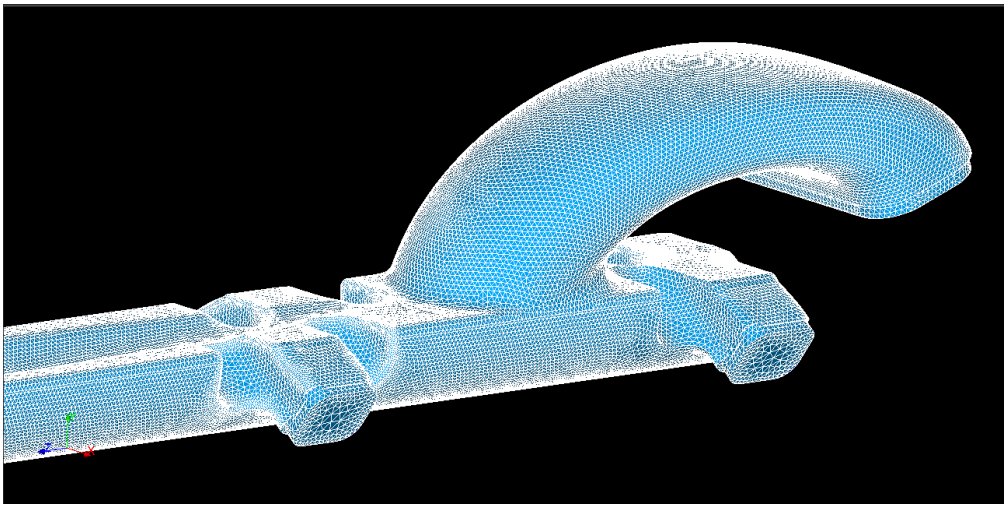


Figure 4: Water channel meshed in SALOME

Toute information contenue dans ce document est libre d'être diffusée à des tierces parties.

Simulation in OpenFoam

The model was simulated using an inlet velocity U of 2.8 m/s normal to the inlet face, a kinetic energy dissipation factor ε of 5.3, a kinetic energy factor k of 0.05, and a surface roughness factor Ks of 63 µm.

The Kepsilon turbulence model was used, and the whole thing was solved with the SimpleFoam model.

Results analysis

Analysis of the hydraulic flux

Here are the results of the simulation:

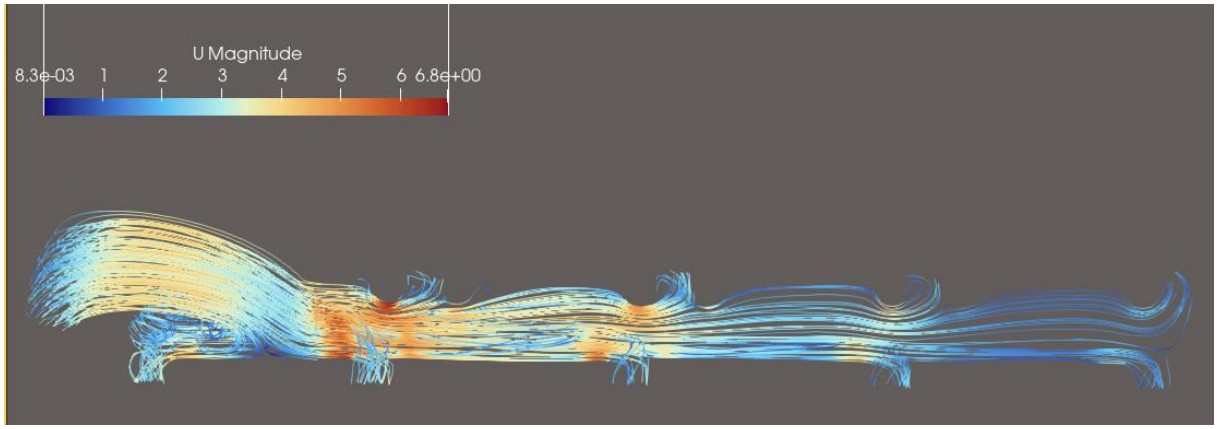


Figure 5: Field lines of the hydraulic flux

We can see that the hydraulic field lines are not visually broken and do not create eddies, except at the left end of the channel where a slight recirculation appears. The problem could certainly be solved by slightly modifying the geometry (creating a central pocket forcing the water to flow towards the sides, i.e. towards the cylinder inlets), but the channel is already sound as it is.

There is also a local increase in speed (orange and red areas) at the pockets for the screws to pass through, but these “baffles” do not break the flow.

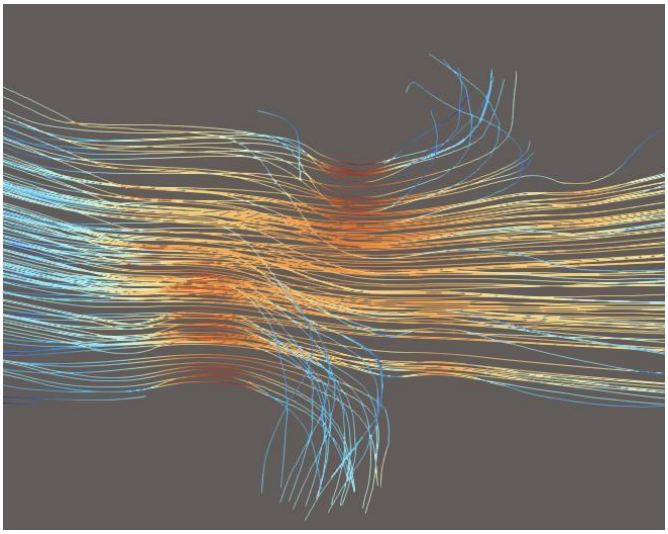


Figure 6: Local acceleration of the flux

No significant depression is observed throughout the channel, including locally in sensitive areas.

Toute information contenue dans ce document est libre d'être diffusée à des tierces parties.

Since the evaporation pressure of water at 90°C is 70 kPa absolute, our system, with maximum local losses of 39 kPa at an inlet pressure greater than 200 kPa (2 bar), remains well above this value.

It is therefore highly unlikely that the flow of fluid in the channel will cause cavitation. Please note that the scale in Figure 7 does not show the total pressure in the circuit, but rather the pressure differentials between the different areas of the channel.

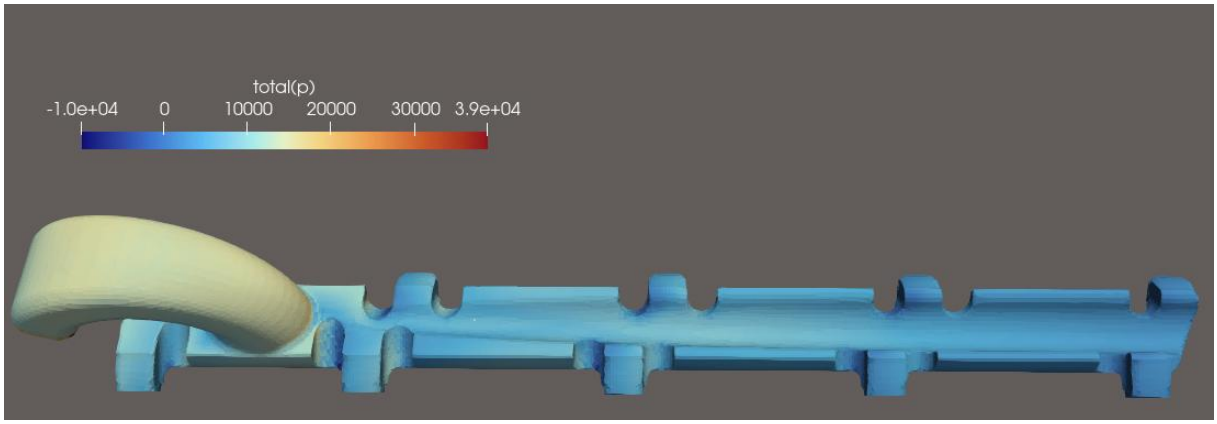


Figure 7: Relative pressure gradient in the channel

Analysis of the pressure differential between cylinders

Using the ParaView visualization tools, we can extract the pressure at the channel outlets (grouped between adjacent cylinders for greater clarity).

We obtain the following results:

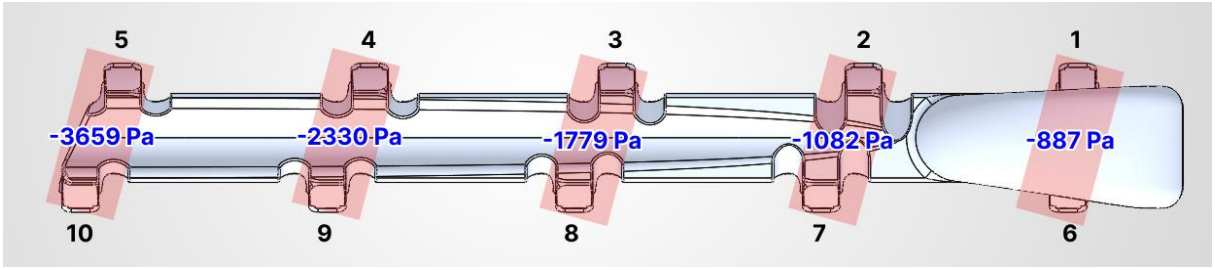


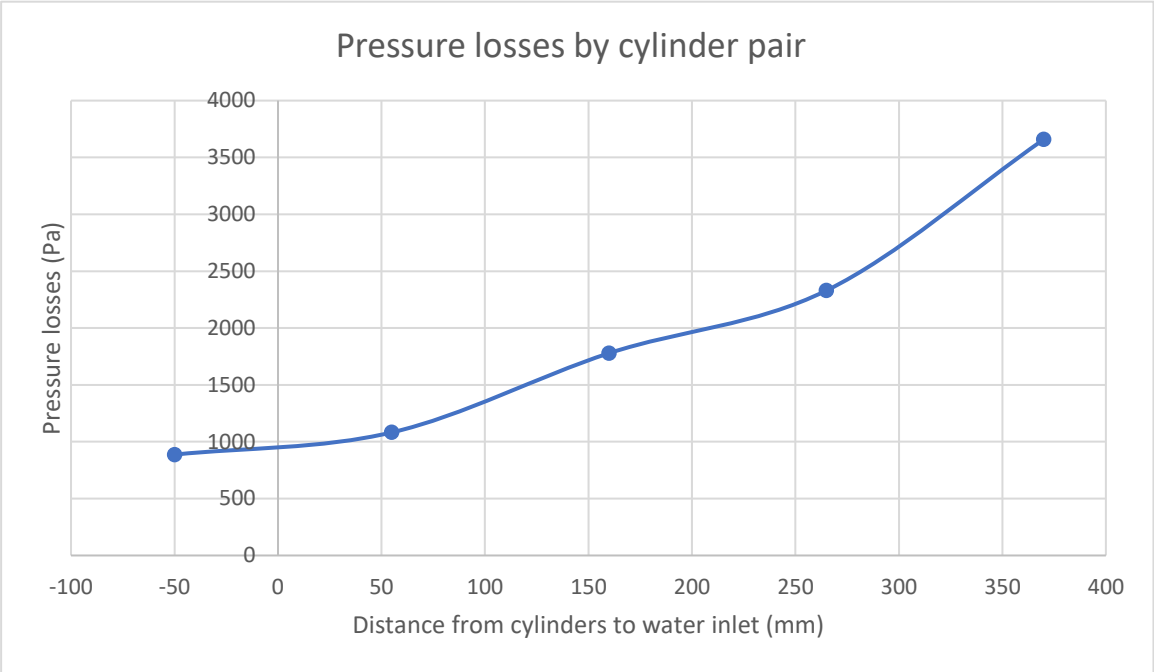
Figure 8: Pressure difference between each pair of cylinders

Since the total pressure supplied by the pump is set at 2.5 bar, or 250 kPa, we will use an initial total pressure of 200 kPa to simulate a degraded system and consider the pressure losses accumulated between the pump and the channel, through the engine block. Under these conditions, the pressures distributed to the cylinders are:

Cylinder numbers	Distance to water arrival point [mm]	Pressure drop per cylinder [Pa]	Estimated pressure by cylinder [kPa]
Cylinders 1-6	-50	887	199,1
Cylinders 2-7	55	1082	198,9
Cylinders 3-8	160	1779	198,2
Cylinders 4-9	265	2330	197,7
Cylinders 5-10	370	3659	196,3

Toute information contenue dans ce document est libre d'être diffusée à des tierces parties.

The estimated pressure per cylinder corresponds to the total pressure remaining locally, obtained by subtracting local pressure losses from the assumed inlet pressure of 200 kPa.



The ΔP_{max} between the cylinders is therefore approximately 2.8 kPa, or approximately 0.03 bar, which represents a maximum pressure imbalance of 1.5% between the cylinders. This value is below the target of 5%. Furthermore, the pressure drop curve does not show any sudden increase in pressure drops towards the end of the channel. The increase in pressure drops from 300 mm from the entry point is directly related to the gradual reduction in the effective hydraulic cross-sectional area and the increase in the ratio between contact surfaces of the fluid and the channel, and the local volume of the fluid.

Conclusion

The CFD simulation of the water distribution channel shows an overall pressure drop of around 3.5 kPa at nominal flow rate, indicating a geometry with little hydraulic penalty and an even distribution of pressure between the cylinders. This value is consistent with the orders of magnitude expected for this type of circuit and confirms that most of the manometric height provided by the pump will be consumed by the rest of the system.

This validation allows the geometry of the channel to be fixed without any negative impact on the sizing of the water pump, leaving a comfortable margin for pressure losses induced by the block, cylinder heads, and heat exchangers.

Toute information contenue dans ce document est libre d'être diffusée à des tierces parties.

Initial sizing of the water pump

Let's start by reviewing the initial values:

The target flow rate is 267 L/min = 0.00445 m3/s. Maximum power is delivered at 10,500 rpm. With a speed ratio between the pump and the crankshaft of 0.581, the pump speed at the high point is 6,100 rpm. The total manometric height targeted at 267 L/min is approximately 25 m.

With these values, we can pre-dimension our pump for initial CAD.

Construction of a water pump

The principle of a water pump is as follows:

Water or other low-viscosity liquid enters the pump at a certain flow rate through the inlet, located in the center of the rotor. The water is accelerated by the impeller and then expelled into the volute (export/outlet).

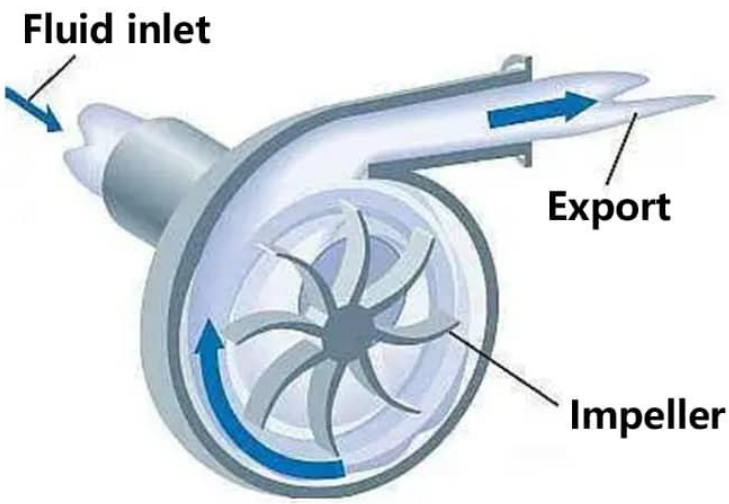


Figure 9: Generic illustration of a water pump

The flow rate is generated by the action of the pump but also by the system. Each hydraulic system has a unique geometry and its own flow rate, depending on the speed of rotation of the pump. At this flow rate, the pump will generate a certain pressure differential between the inlet and outlet. By converting this pressure differential into water column height (by dividing the pressure in Pascals by the gravity and density of the fluid, 10447 in our case), we obtain the pump's performance in meters.

We start by pre-sizing the pump using mathematical formulas, then we simulate the flow of fluids in the 3D model to obtain a value representative of reality and optimize until we obtain the desired performance. Once the design has been established, simulations are carried out at different flow rates to determine the pump's performance curve: manometric height as a function of flow rate. This curve will indicate whether the pump will perform well in all cases of use.

Toute information contenue dans ce document est libre d'être diffusée à des tierces parties.

Choice of overall design

By calculating the specific speed of the pump, we can determine which class it will belong to, which will allow us to choose a type of impeller (rotor) that is suitable for our application.

The specific speed of a pump is given by : $N_s = N * \frac{\sqrt{Q}}{\sqrt[4]{H^3}}$ with :

$$N = Rotation\ speed\ \left[\frac{tr}{min}\right];$$

$$Q = Fluid\ flow\ rate\ \left[\frac{m^3}{s}\right];$$

$$H = Total\ manometric\ height[m]$$

In our case, $N_s = 6100 * \frac{\sqrt{0.00445}}{\sqrt[4]{25,5^3}} \sim 36$

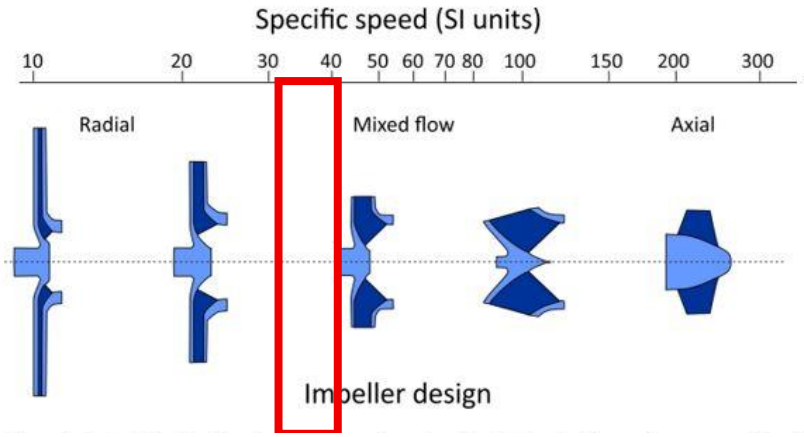


Figure 10: Typical suction speed values for various impeller designs

The figure below shows the appropriate pump designs for specific speeds. With a specific speed of 36, our pump is between mixed flow and radial flow.

The pump design will therefore have a relatively small axial dimension and a relatively large rotor diameter. The ratio between diameter and width will be between 3:1 and 6:1.

Rotor pre-dimensioning

To generate sufficient overpressure, the pump must accelerate the liquid to a sufficient speed to reach a pressure of 2.5 bar, or what corresponds to a total manometric height of 25 m.

The fluid accelerated by the pump will reach its maximum speed at the maximum diameter of the rotor, at the blade outlet. The diameter of the rotor therefore has a decisive influence on the outlet speed of the fluid and, ultimately, on the pressure differential generated.

The formula used to define the speed of the fluid U at the end of the rotor based on the manometric height is as follows:

Toute information contenue dans ce document est libre d'être diffusée à des tierces parties.

$$HMT = \psi * \frac{U^2}{2g} \rightarrow U = \sqrt{\frac{2gH}{\psi}} = \sqrt{\frac{2 * 9{,}81 * 25}{0{,}9}} = 23{,}3\ m/s$$

With ψ local hydraulic efficiency ~0.9: This value corresponds to typical local hydraulic efficiency for a properly sized centrifugal pump, excluding volute losses and leaks.

From the equation linking the required peripheral velocity of the fluid and the geometry of the rotor, we can extract the diameter of the latter: $U = \frac{\pi DN}{60}$ (with D in mm)

Rotor diameter: $D = \frac{60U}{\pi n} = \frac{60*23{,}3}{\pi*6100} \sim 73mm$

This diameter is standard for this category.

The height of the blade is chosen at a ratio of approximately 1/5 of the diameter, at 15 mm.

Pre-dimensioning the water inlet

To avoid cavitation (local phase change of the fluid with transformation into gas), the pressure must be sufficient throughout the circuit, including at the pump inlet. The fluid flow velocity must therefore be limited. Here, a value of 3 m/s has been chosen as the upper limit.

If we want an inlet velocity into the pump of 2.5 m/s, we will need the following cross-sectional area:

$$S_{inlet} = \frac{Q}{V_{inlet}} = \frac{0{,}00445}{2{,}5} = 0{,}00178\ m^2$$

If we use this value of 0.00178 m^2 to define the inlet diameter, we obtain:

$$D_{inlet} = \sqrt{4 * \frac{S_{inlet}}{\pi}} = \sqrt{4 * \frac{1780}{\pi}} \sim 48\ mm$$

Therefore, the diameter of the inlet will be 48 mm.

Pre-dimensioning of the outlet section and volute

The same logic of speed in relation to flow rate applies at the outlet, to determine the cross-section at the end of the volute. However, as the pump is located at the lowest point of the engine, the size of the volute directly affects the height of the crankshaft in relation to the floor, and therefore the center of gravity of the engine and the vehicle. It is therefore necessary to find a compromise between the cross-section and the overall dimensions of the assembly.

By choosing a section profile of 50*31.5 mm with 4 mm fillets on the edges, we obtain a section of:

$$S_{out} = 50 * 31{,}5 - 4^2\pi \sim 1524\ mm^2$$

These dimensions were chosen after several tests and represent a good compromise between section size, section proportions, and space requirements in the casing.

To ensure gradual acceleration of the fluid at the rotor outlet and good flow, the volute must have a “shell” shape, starting from an initial zero section and gradually enlarging towards the outlet section. The

Toute information contenue dans ce document est libre d'être diffusée à des tierces parties.

section can increase according to linear or exponential law. To limit the size of section S_2, which determines the distance between the crankshaft and the floor (located at the bottom of the volute), a linear law is chosen.

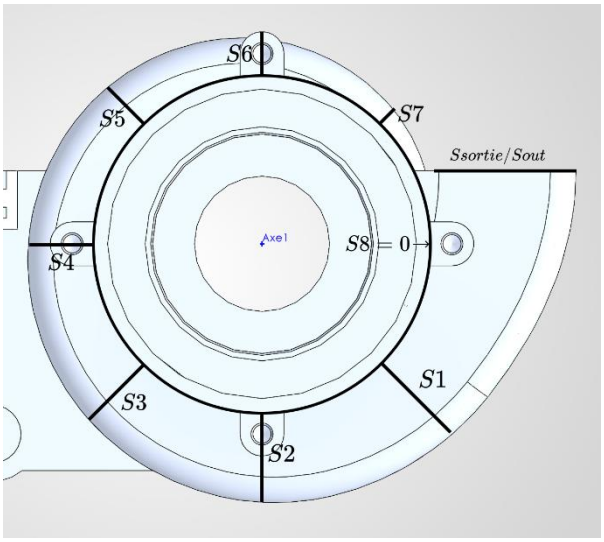


Figure 11: Sections of the volute

Once the outlet section has been determined, the following sections are deduced using the linear evolution law applied to each eighth of the volute:

$$S_n = \frac{(8-n)S_{out}}{8}$$

By setting the size of the sections and the length L, we can find the width l. Here, the length L_{out} (normal to the following diagram) is set at 50 mm for the section S_{out}, and decreases by 2 mm for each eighth of the volute. By design, there are only three 4 mm radius fillets and not four on these sections.
Thus, each width is given by the following formula:

$$\forall n \in [1;7], \qquad l_n = \frac{S_n + \frac{3}{4}\pi 4^2}{L_n} = \frac{\frac{(8-n)S_{out}}{8} + \frac{3}{4}\pi 4^2}{L_{out} - 2n}$$

The results of this equation give us the table below:

Section name	Section size [mm^2]	Length [mm]	Width [mm]
S_{out}	1524	50	31.5
S_1	1333.5	48	28.6
S_2	1143	46	25.7
S_3	952.5	44	22.5
S_4	762	42	19
S_5	571.5	40	15.2
S_6	381	38	11
S_7	190.5	36	6.3
S_8	~0	34	~0

Toute information contenue dans ce document est libre d'être diffusée à des tierces parties.

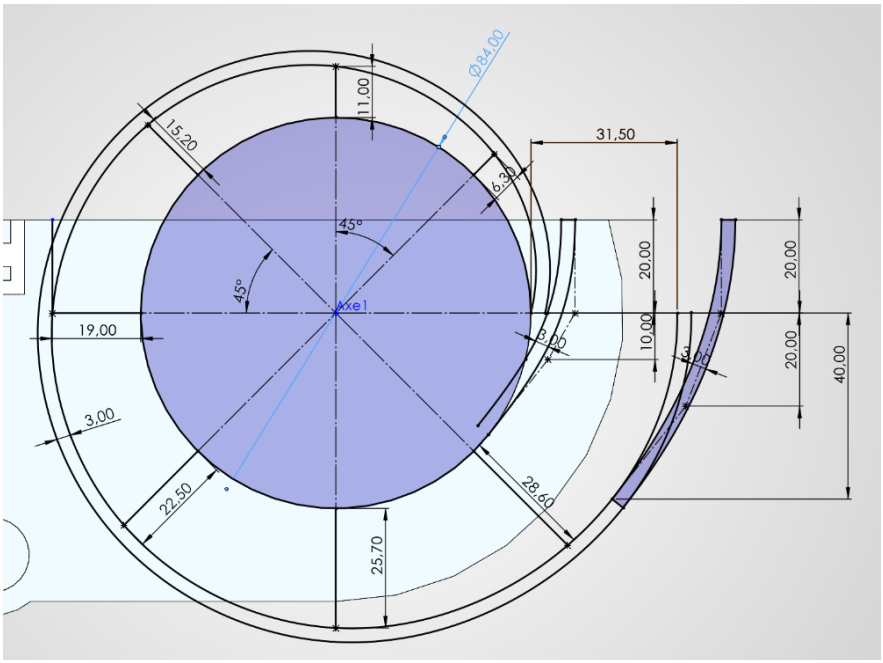


Figure 13: Values of the volute sections

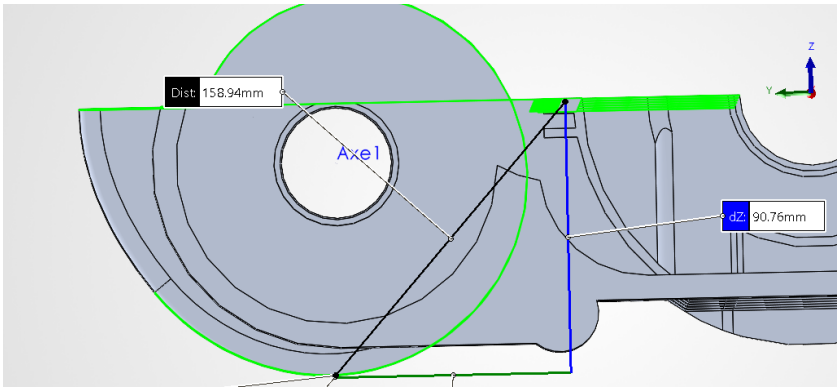


Figure 12: Distance from the bottom of the volute (Section 2) to the center of the crankshaft

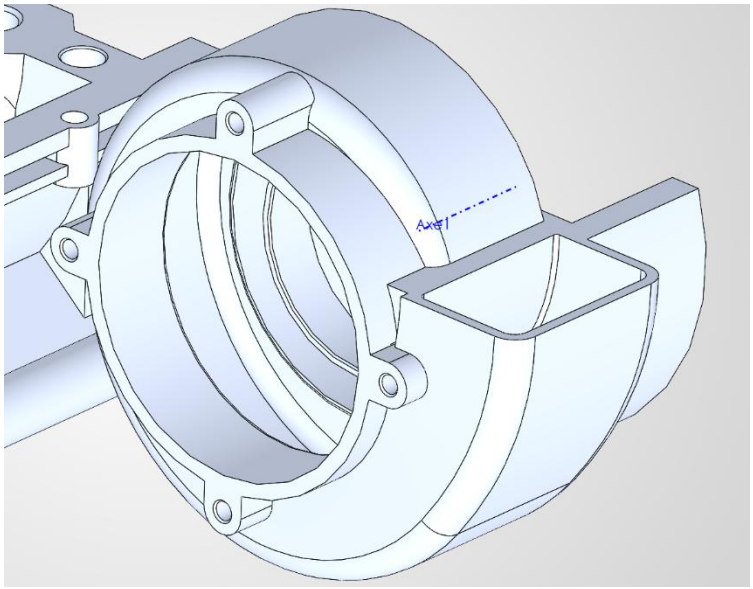


Figure 14: 3D model of the pump body

Toute information contenue dans ce document est libre d'être diffusée à des tierces parties.

Preparation of the model for CFD

Once pre-dimensioned, the pump was modeled in Solidworks, then tested and iterated using the results obtained with OpenFoam.

It is divided into three areas:

- Inlet
- Impeller
- Volute

The inlet represents the water inlet into the rotor area. It is divided into three parts:

- ***inlet1***, the area where the fluid enters the pump
- ***wall1***, the walls of the area
- ***AMI1_1***, the interface between the inlet and the rotating area, the impeller.

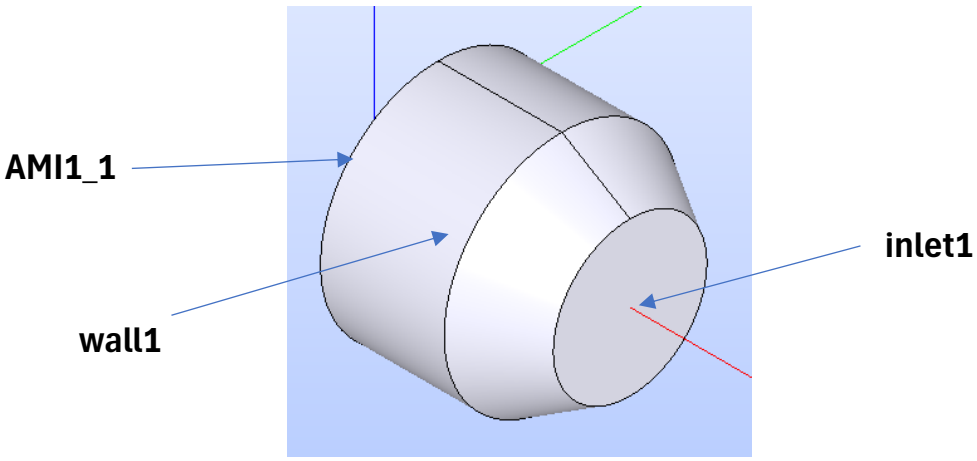


Figure 15: CFD model ofthe water inlet

The impeller represents the rotating volume driven by the pump rotor. It is divided into:

- ***AMI1_2***, the interface with the inlet
- ***wall2***, the walls of the area (simplified model to keep the mesh simple)
- ***AMI2_1***, the interface with the volute

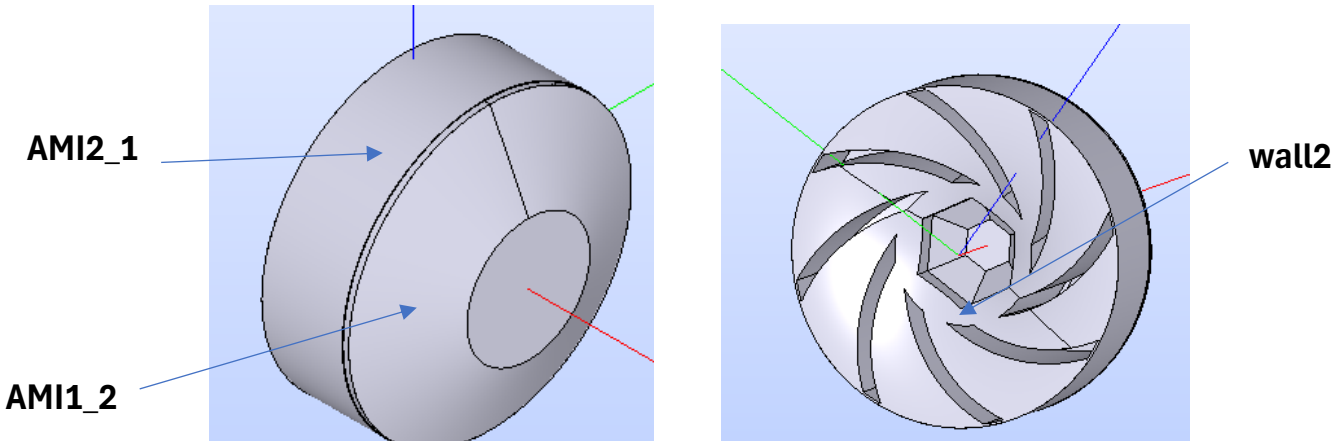


Figure 16: CFD model of the rotor

Toute information contenue dans ce document est libre d'être diffusée à des tierces parties.

The volute represents the fluid outlet channel, located after the rotor in the circuit. It is divided between:

- ***AMI2_2***, the interface with the impeller
- ***wall3***, the walls of the area
- ***outlet1***, the fluid outlet

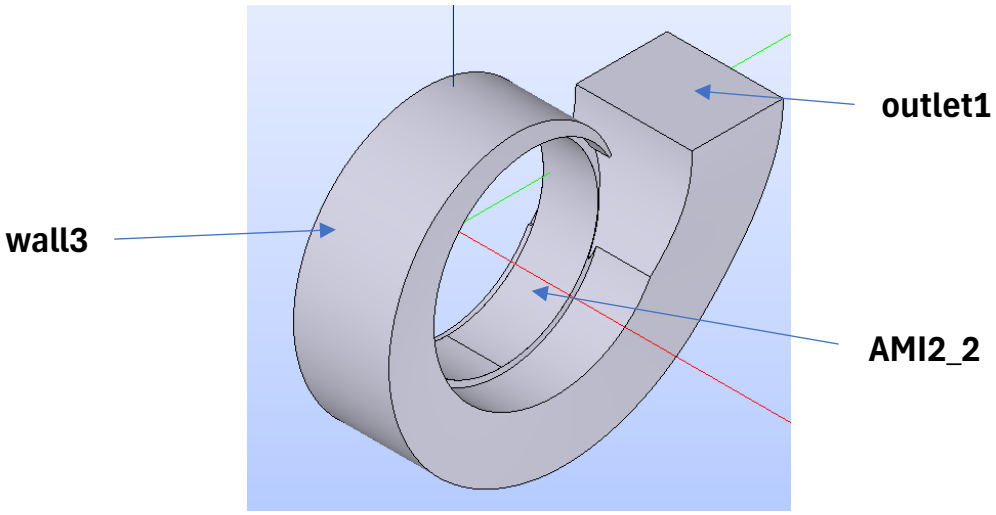


Figure 17: CFD model of the volute (outlet)

meshing in SALOME

The pump was meshed according to the following parameters (in mm):

Dimension	Algorithm	Max. Size	Min. Size
3D	NETGEN 3D	0.002	0.00005
2D	NETGEN 2D-1D	0.002	0.00005
1D	NETGEN 2D-1D	0.002	0.00005

A local refinement of 0.001 mm was applied to the walls of the model.

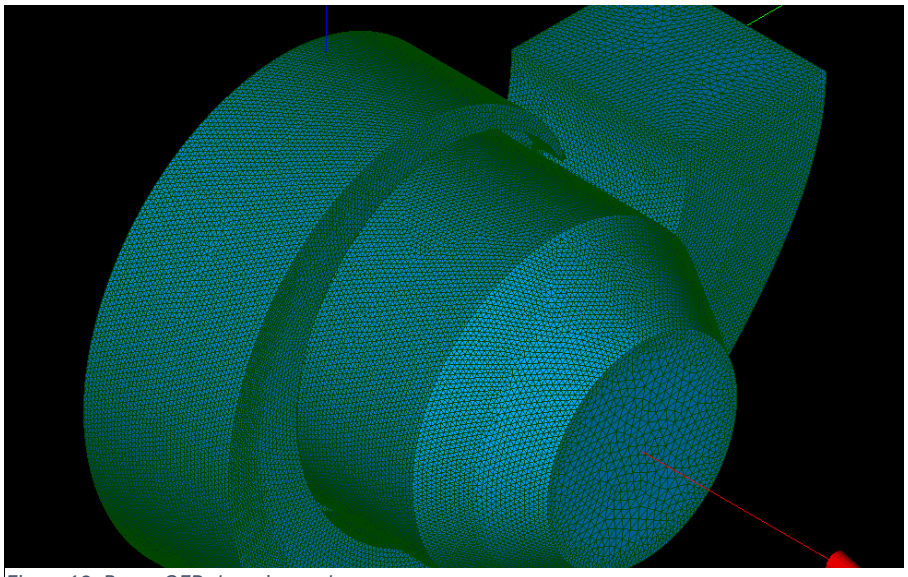


Figure 18: Pump CFD domain mesh

Toute information contenue dans ce document est libre d'être diffusée à des tierces parties.

Simulation in OpenFoam

The inlet flow rate U is set at 0.00445 m^3/s (267 L/min), the fluid density ρ at 1065 kg/m^3, the rotor speed Ω at 638.8 rad/s (6100 rpm), surface roughness R_s is set at 63 µm, the kinematic viscosity of the fluid ν is set at 1.69 × 10^{-6} m^2/s, the turbulence intensity T_u is set at 5%, and the Eddy viscosity ratio is set at 10.

The values derived from these initially defined conditions are as follows:

Parameter	Symbol	Value
Pressure/density	P	95,1408
Specific turbulence dissipation rate	ω	1866,124
Kinetic energy of turbulence	k	0,0315375
Turbulence dissipation	ϵ	5,2968

$\omega, k\ and\ \epsilon$ ϵ were calculated using Wolfdynamics' online calculator:

Wolfdynamics calculator, *choose « Compute turbulence variables (κ, ϵ, ω) from Tu, μt/μ, U∞ and kinematic viscosity ν »*

Note: ϵ is not used in the chosen model but was used to calculate turbulence in the water distribution channel studied at the beginning of this document.

The turbulence model used is KOmegaSST, and the solver is SimpleFoam.

To quantify the pump's performance, we need to find the total manometric height HMT, which depends on the overpressure generated by the pump ; in other words, the pressure differential between the inlet and outlet. Using the "integrate variables" tool in the ParaView viewer, it is possible to retrieve the pressure on each of these surfaces.

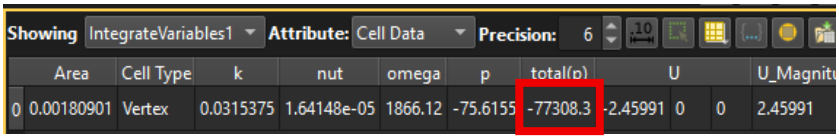


Figure 19: Inlet and outlet total pressure, calculated on ParaView

By applying the wollowing formula:

$$HMT = \frac{P_{out} - P_{inlet}}{\rho g}$$

We obtain the total manometric height of the pump. As a reminder, our objective is to reach approximately 25 m at a flow rate of 267 L/min, knowing that this value is oversized by 20%.

Toute information contenue dans ce document est libre d'être diffusée à des tierces parties.

First, second and third try

Critical values of the rotor:

Rotor diameter (mm)	74
Useful height of the rotor (mm)	15
Rotor speed (rpm) [rad/s]	6100 [638,8]
Blade entry angle of attack (°)	35
Blade exit angle of attack (°)	40

The simulation gave us the following results:

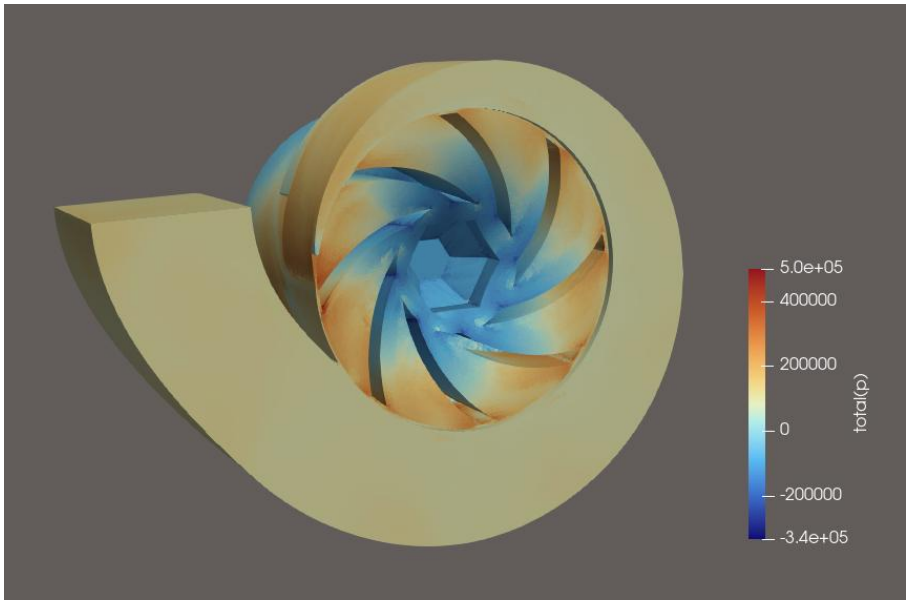


Figure 20: Total pressure in the pump, results of the first simulation

$HMT = \frac{109409-(-77308)}{1065*9.81}$ = 17,9 m.

The value is well below the expected 25 m, so the geometry is reviewed successively according to several dimensions: increase in speed, increase in rotor diameter, modification of the blade exit angle.

A second simulation carried out by optimizing the geometry (reducing the size of the central nut, blades extending more towards the center) resulted in a modest increase in HMT to 18.2 m.

In Article 1 on the V1046AA, we chose a water pump reduction ratio relative to the crankshaft of 0.581, with this combination of gears:

$$R_{water}Z39 = \frac{34}{42} * \frac{28}{25} * \frac{25}{39} = 0{,}581$$

To slightly increase the speed, the gear attached to the pump shaft now has 38 teeth, for a reduction ratio of 0.596.

$$R_{water}Z38 = \frac{34}{42} * \frac{28}{25} * \frac{25}{38} = 0{,}596$$

Thus, at maximum power output of 10,500 rpm, the pump runs at 6,258 rpm instead of 6,100 rpm.

Toute information contenue dans ce document est libre d'être diffusée à des tierces parties.

The simulation is therefore repeated with:

Rotor diameter (mm)	74
Useful height of the rotor (mm)	15
Rotor speed (rpm) [rad/s]	6258 [655,3]
Blade entry angle of attack (°)	35
Blade exit angle of attack (°)	40

We get: $HMT = \frac{109396-(-91179)}{1065*9.81}$ = 19,2m

Thus, with a 2.6% increase in rotational speed, we obtained a 1m increase in HMT, or 5.5%.

Increase in rotor size and modification of blade angle of attack

The fourth simulation reuses the previous data, increasing the rotor diameter from 74 mm to 80 mm.

According to theory, the manometric height is related to the fluid outlet velocity by the following formula:

$$HMT = \psi * \frac{U^2}{2g}$$

However, U is related to D by the following relationship:

$$U = \frac{\pi DN}{60}$$

Thus, a linear increase in diameter should result in a quadratic increase in total manometric height. (It is interesting to note the same relationship with the rotor speed, confirmed in the previous example).

The simulation is repeated with the following parameters:

Rotor diameter (mm)	80
Useful height of the rotor (mm)	15
Rotor speed (rpm) [rad/s]	6258 [655,3]
Blade entry angle of attack (°)	35
Blade exit angle of attack (°)	40

We obtain: $HMT = \frac{109413-(-125742)}{1065*9.81}$ = 22,5m.

Thus, with an 8.1% increase in diameter, we increased the HMT by 17.2%, which corresponds to the expected values.

Subsequently, various modifications were made to the blade exit angle, tested at 25°, 45°, 48°, and 50°. The simulations were conducted without modifying the other parameters. The results are as follows:

Angle (°)	25	40	45	48	50
HMT (m)	20,9	22,5	23	22,9	39 (!)

Toute information contenue dans ce document est libre d'être diffusée à des tierces parties.

Since the HMT value at 50° is most likely due to a simulation convergence error, it will be ignored. Thus, the ideal exit angle for our application is 45° and will be used thereafter.

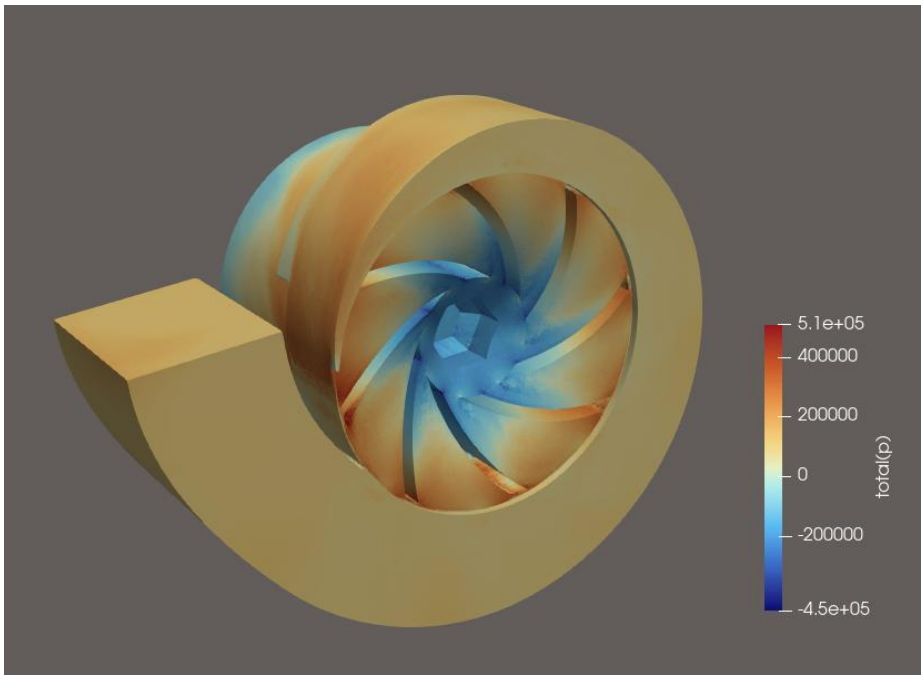


Figure 21: Simulation results after optimization

Simulation for validation of general parameters

Taking all these improvements into account, the diameter is increased by 5% to bring the HMT to the expected 25m. Thus, it increases from 80 to 84mm.

The simulation is repeated with:

Rotor diameter (mm)	84
Useful height of the rotor (mm)	15
Rotor speed (rpm) [rad/s]	6258 [655,3]
Blade entry angle of attack (°)	35
Blade exit angle of attack (°)	45

We obtain:

$HMT = \frac{111203-(-144748)}{1065*9.81}$= 24,5m, this represents an increase of 6.5%, which is rather disappointing compared to expectations.

However, further increasing the rotor diameter would mean increasing the size of the volute, and therefore the height of the crankshaft above the ground, the center of gravity of the motor, and the entire vehicle. The reduction ratio of the pump relative to the crankshaft is already high, and switching to a 37-tooth gear would mean switching to a ratio >0.6. It is no longer possible to optimize the angle of the blades, and increasing the effective height of the rotor would increase the axial dimension of the pump, which is possible but not optimal for the hybrid system behind it, which will be the subject of a future article.

Toute information contenue dans ce document est libre d'être diffusée à des tierces parties.

It is also interesting to note that the surface roughness is 63 µm, equivalent to the roughness of sand casting, while certain components such as the rotor will be machined, with a roughness of <3.2 µm, greatly limiting pressure losses.

Furthermore, since the value of 25 m for HMT is 20% oversized, 24.5 m is acceptable. It would also be useful to repeat the simulation several times to confirm this value.

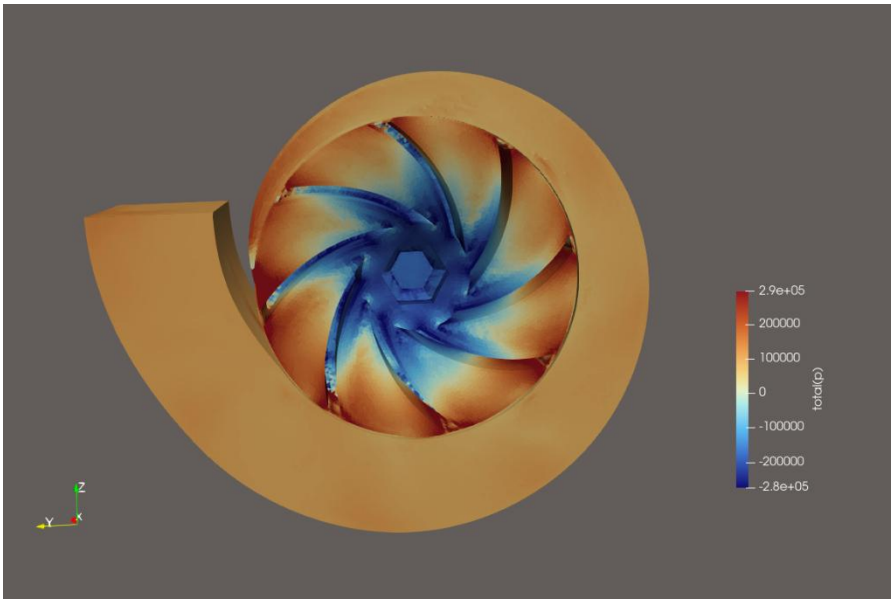


Figure 22: Simulation results, final parameters

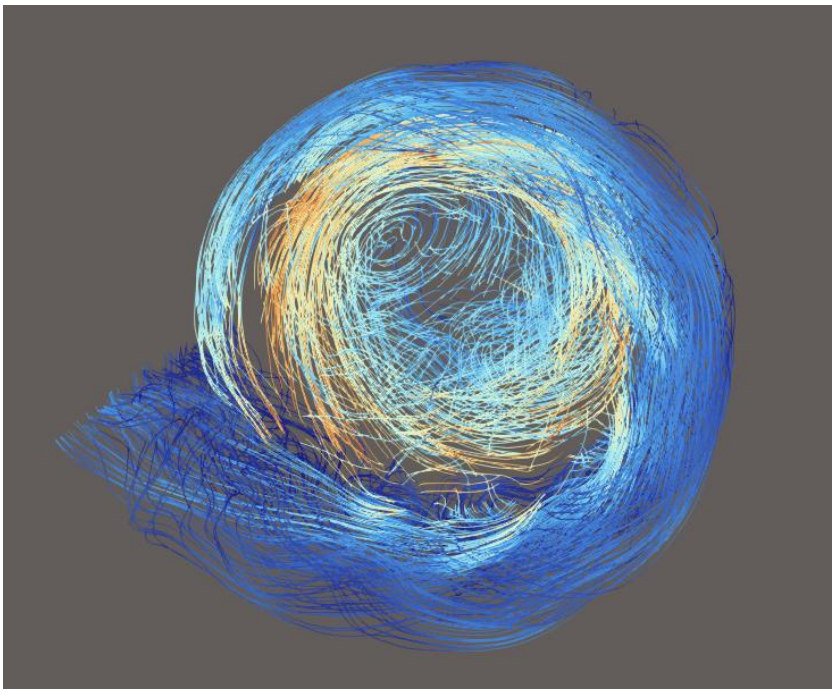


Figure 23: Hydraulic field of the last simulation

Toute information contenue dans ce document est libre d'être diffusée à des tierces parties.

The force applied to the axis of rotation is 741 N, the moment is 17.4 Nm.

```
forces forces write:
    Sum of forces
        Total    : (741.267 13.182 4.24234)
        Pressure : (746.513 12.518 4.03908)
        Viscous  : (-5.24659 0.66395 0.203263)
    Sum of moments
        Total    : (-17.419 0.672958 1.18167)
        Pressure : (-17.0206 0.683094 1.16794)
        Viscous  : (-0.398379 -0.0101352 0.0137292)
    writing force and moment files.
```

Figure 24: Hydraulic force on the rotating shaft

```
496            -1.744106e+01 6.787027e-01 1.181089e+00 -
497            -1.743360e+01 6.773811e-01 1.181393e+00 -
498            -1.742630e+01 6.754267e-01 1.181484e+00 -
499            -1.741901e+01 6.729584e-01 1.181672e+00 -
500            -1.741169e+01 6.702028e-01 1.182337e+00 -
```

Figure 25: Moment applied on the rotating shaft

Thus, we can find the effective radius of application of the torque:

$$r_{app}[mm] = \frac{C}{F} * 1000 = \frac{17{,}4}{741} * 1000 = 23{,}5\ mm$$

That is to say, the combined action of the fluid on the rotor is equivalent to a torque applied to a point located on a circle with a diameter of 47 mm.

We can find the power:

$$P = C\omega = 17{,}4 * 655{,}3 = 11402\ W = 11{,}4\ kW$$

Toute information contenue dans ce document est libre d'être diffusée à des tierces parties.

Conclusion

The study of the V1046AA cooling circuit validated both the hydraulic distribution to the cylinders and the overall sizing of the water pump.

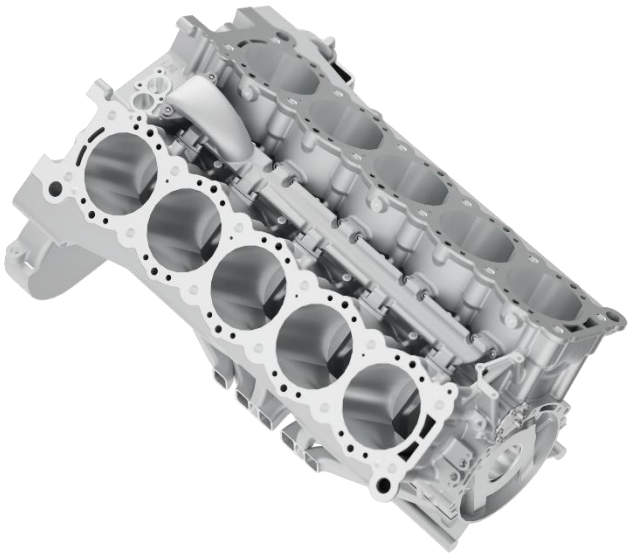
The CFD simulation of the distribution channel confirms a homogeneous pressure distribution between the cylinders, with a maximum imbalance of less than 2% and negligible pressure losses in relation to the total manometric height of the system. This validation allows the geometry of the channel to be fixed without additional constraints on the pump sizing.

The pre-sizing and then numerical optimization of the water pump show that a manometric height of close to 25 m can be achieved at a nominal flow rate of 267 L/min, with an absorbed power of around 11 kW. The results obtained are consistent with centrifugal pump theory and confirm the validity of the initial assumptions.

Despite a slight deviation from the initial oversized target, the performance achieved is considered sufficient given the margins retained for roughness, pressure losses in the rest of the circuit, and actual operating conditions. The geometry selected thus provides a sound basis for the final mechanical integration of the pump into the engine.

The next steps will focus on the final assembly of the pump with its re-optimization, integration with the other engine systems, and the study of the behavior of the cooling circuit in changing conditions.





Toute information contenue dans ce document est libre d'être diffusée à des tierces parties.